

# Medical Image Fusion Using Multiresolution Transforms

Kalpa N. Mori<sup>1</sup> Dr. Komal R. Borisagar<sup>2</sup>

<sup>1</sup>PG Student <sup>2</sup>Asst. Professor

<sup>1,2</sup>AITS, Rajkot

**Abstract**--- Image fusion is used to generate information from multiple images of the same scene to get a composite image that is more suitable for image-processing tasks i.e. Surveillance, Medical applications. In this paper the multi-source medical images like MRI (Magnetic Resonance Imaging), CT (computed tomography) & PET (positron emission tomography) are fused using different multi scale transforms. We compare various multi resolution transform algorithms, especially the latest developed methods, such as; Non Subsampled Contourlet Transform, Fast Discrete Curvelet, Contourlet, Discrete Wavelet transform for image fusion. The fusion operations are performed with all Multi resolution transforms. The fusion rules like local maxima and spatial frequency techniques are used for selection in the low frequency and high frequency sub band coefficients, which can preserve more information and quality in the fused image. The fused output obtained after the inverse transform of fused sub band coefficients. The experimental results show that the effectiveness of fusion approaches in fusing multi source images.

**Keywords:** Image Fusion; Discrete Wavelet Transform; Contourlet Transform; Fast Discrete Curvelet Transform; Non subsampled Contourlet Transform.

## I. INTRODUCTION

The Image fusion is used to generate the process of combining information from two or more images of a scene into a single composite image which is more informative and is more suitable for image Processing Applications. The objective in the image fusion is to reduce uncertainty and minimize redundancy in the output, while maximizing relevant information particular to an application or task as well. Given the same set of input images, different fused images may be created depending on the specific application and what is considered as relevant information. There are several benefits in using image fusion: wider spatial and temporal coverage with decreased uncertainty, improved reliability and increased robustness of system performance [3].

The medical images like MRI and CT provides high-resolution images with structural and anatomical information. PET images provide functional information with low spatial resolution. In the recent years, the success of MRI-CT, PET-MRI [1] & PET-CT [6] imaging in the clinical field triggered considerable interest in noninvasive functional and anatomical imaging. The limited spatial resolution in PET images is often resulted unsatisfactory in morphological analysis. Combining anatomical and functional tomography datasets provide much more qualitative detection and quantitative determination in this area [1] & [10].

So far, several fusion algorithms based on multi source medical images have been proposed. The MRI-CT image fusion using edge preserved technique proposed by Xianghi et al, based on multi scale toggle contrast operator [4]. The MRI-PET image fusion proposed by Sabalan Daneshvar et al based on combining HIS (Hue Intensity Saturation model) and retina models improve the functional and spatial information content [1]. The CT-PET image fusion proposed by Yuhui Liu et al, based on multi wavelet transform adds more details and structure information [6].

The rest of the paper is organized as follows: Section 2 explains Multiscale transforms. Section 3 the discussion on the experimental results. In the laconic section, the paper is concluded.

## II. MULTIREOLUTION TRANSFORMATIONS

### A. Discrete Wavelet Transform

Discrete Wavelet transform (DWT) provides a framework in which a signal is decomposed, with each level corresponding to lower frequency sub band, and higher frequency sub bands. There are two main groups of transforms: continuous and discrete. In one dimension the idea of the wavelet transform is to present the signal as a superposition of wavelets. If a signal is represented by  $f(t)$ , the wavelet decomposition is

$$f(t) = \sum_{m,n} c_{m,n} \Psi_{m,n}(t) \tag{2.1}$$

, Where  $\Psi_{m,n}(t) = 2^{-m/2} \psi(2^{-m}t - n)$ ,  $m$  and  $n$  are integers. There exist very special choices of  $\Psi$  such that  $\Psi_{m,n}(t)$  constitutes an ortho normal basis, so that the wavelet transform coefficient can be obtained by an inner calculation:

$$c_{m,n} = \langle f, \Psi_{m,n} \rangle = \int \Psi_{m,n}(t) f(t) dt \tag{2.2}$$

In order to develop a multiresolution analysis, a scaling function  $\phi$  is needed, together with the dilated and translated

Parameters of  $\phi_{m,n}(t) = 2^{-m/2} \phi(2^{-m}t - n)$ . The Signal  $f(t)$  can be decomposed in its coarse part and details of various sizes by projecting it onto the corresponding spaces.

Therefore, the approximation coefficients  $A_{m,n}$  of the function  $f$  at resolution  $2^m$  and wavelet coefficient  $C_{m,n}$  can be obtained:

$$a_{m,n} = \sum_k h_{2n-k} a_{m-1,k} \quad (2.3)$$

$$c_{m,n} = \sum_k g_{2n-k} a_{m-1,k} \quad (2.4)$$

Where  $h_n$  is a low pass FIR filter and  $g_n$  is a high pass FIR filter. To reconstruct the original signal, the analysis filter can be selected from a biorthogonal set which have a related set of synthesis filters. These synthesis filters can be used to perfectly reconstruct the signal using the reconstruction formula:

$$a_{m-1,l}(s) = \sum_n [\tilde{h}_{2n-l} a_{m,n}(s) + \tilde{g}_{2n-l} c_{m,n}(s)] \quad (2.5)$$

Equations (2.3) and (2.4) are implemented by filtering and down sampling. Conversely equation (2.5) is implemented by an initial up sampling and a subsequent filtering.

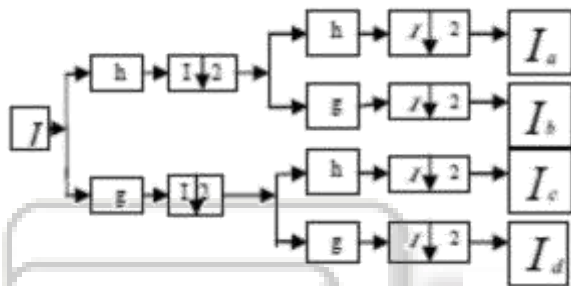


Fig. 1: Structure of 2-D DWT

In a 2-D DWT, a 1-D DWT is first performed on the rows and then columns of the data by separately filtering and down sampling. This result in one set of approximation coefficients  $I_a$  and three set of detail coefficients, as shown in Fig 1, Where  $I_b, I_c, I_d$  represent the horizontal, vertical and diagonal directions of the image I, respectively.

In the filter theory, these four sub images correspond to the outputs of low-low (LL), low-high (LH), high-low (HL), and high-high (HH) bands. By recursively applying the same scheme to the LL sub band multi resolution decomposition with a desire level can then be achieved. There, a DWT with K decomposition levels will have  $M=3*K+1$  such frequency bands.

### B. Contourlet Transform

The contourlet transform is first developed in continuous domain and then is discretized for sampled data; contourlet transform starts with a discrete domain construction. The contourlet is also deemed as a “true” two dimensional transform that can capture the intrinsic geometrical structure of an image. Two filter banks are employed to implement the contourlet transform as shown in Fig.2.

The Laplacian pyramid is first used to capture the point discontinuities, and then a directional filter bank is used to link point discontinuities into linear structures. As the DWT, the contourlet transform also has no shift invariant property because of the down-sampling operation.

Do and Vetterli found that to obtain a sparser representation for 2-D piecewise smooth functions in  $R^2$ , an effective method is to utilize a double filter bank scheme, that is, first apply a multiscale decomposition to capture point discontinuities and then perform a local directional

decomposition to synthesize the nearby edge points into independent contour segments.

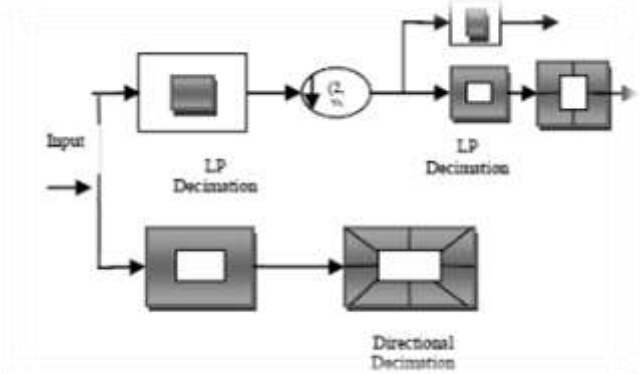


Fig. 2: Block diagram of Contourlet transform

With a rich set of basis oriented at various directions and scales, contourlet can effectively capture the intrinsic contours and edges in natural images that set radiation multiresolution analysis methods are difficult to handle. Contourlet offer s a much richer sub band set of different directions and shapes, which helps to capture geometric structures in images much more efficiently [7].

### C. Non Subsampled Contourlet Transform (NSCT)

In the foremost contourlet transform down samplers and up samplers are presented in both the laplacian pyramid and the Directional Filter Bank (DFB). Thus, it is not shift-invariant, which causes pseudo-Gibbs phenomena around singularities. NSCT is an improved form of contourlet transform. It is motivated to be employed in some applications, in which redundancy is not a major issue, i.e. image fusion. In contrast with contourlet transform, non-subsampled pyramid structure and non-subsampled directional filter banks are employed in NSCT. The non-subsampled pyramid structure is achieved by using two-channel non subsampled 2-D filter banks. The DFB is achieved by switching off the downsamplers/up samplers in each two-channel filter bank in the DFB tree structure and up sampling the filters accordingly. As a result, NSCT is shift-invariant and leads to better frequency selectivity and regularity than contourlet transform. Fig.3 shows the decomposition framework of contourlet transform and NSCT [08]. The NSCT structure consists in a bank of filters that splits the 2-D frequency plane in the subband; these are

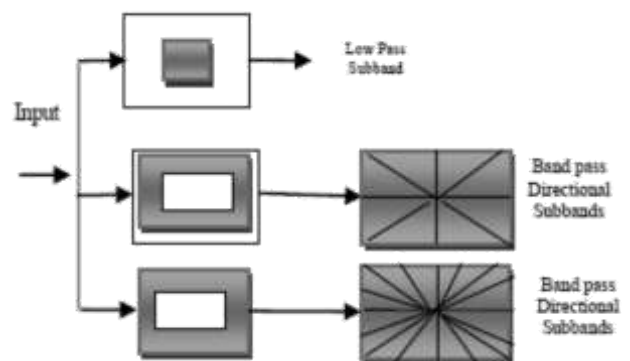


Fig. 3: Block diagram of NSCT

a non-subsampled pyramid structure that ensures the Multiscale property and a non-subsampled directional filter bank structure that gives directionality [09].

#### D. Curvelet Transform

The DWT, SWT, and DTCWT cannot capture curves and edges of images. More reasonable bases should contain geometrical structure information when they are used to represent images. Candes and Donoho proposed the Curvelet transform (CVT) with the idea of representing a curve as a superposition of bases of various lengths of width obeying the scaling width  $\approx$  length. The CVT is referred to as the “true” 2D transform. The discrete version implemented in this is a “wrapping” transform. The second generation of Curvelet transform is presented in Fig. 4. Firstly, the 2D FFT is applied to the source image to obtain Fourier samples. Next, a discrete localizing window smoothly localizes the Fourier transform near the sheared wedges obeying the parabolic scaling. Then, the wrapping transformation is applied to re-index the data. Finally, the inverse 2D FFT is used to obtain the discrete CVT coefficients [8].

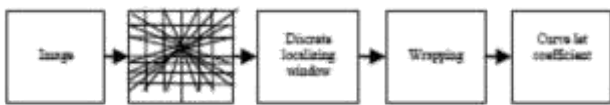


Fig. 4: The second generation of Curvelet transforms

### III. PROPOSED METHOD

In this paper, there are two different input medical source images A and B (like MRI & CT, MRI & PET, CT & PET). The image fusion algorithm should preserve all the salient features of source images. Fig 5 illustrates the generic image fusion frame work based on Multiscale image decomposition methods. The source images are firstly decomposed into low-frequency sub bands and a sequence of high-frequency sub bands in different scales and orientations. Then the fusion coefficients are obtained from sub bands according to fusion rules. Finally, fused image is reconstructed by applying inverse transform on the fused sub bands.

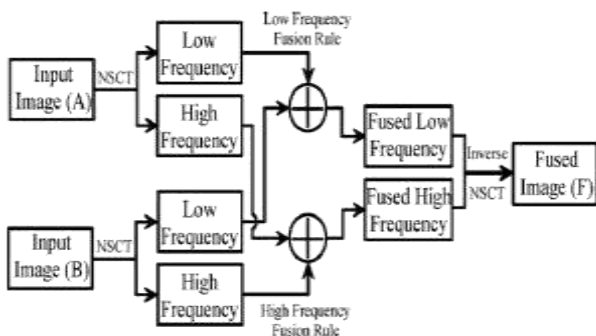


Fig. 5: Block diagram of proposed method

The key issue in spatial domain algorithms is identifying the most important information in source images and fusing the salient information into the fused image [13]. This paper includes the average pixel method and PCA method. The fusion rules are explained in the following sections.

#### A. Fusion rule of lower sub band coefficients

The coefficients in the coarsest scale sub band represent the approximation component of the source image. It is a smooth and sub sampled version of the original image. Therefore, most of the source images information is kept in low frequency bands. The proposed selection principles for

the sub band coefficients are finally defined as the maximum selection rule is:

$$I_L^r(i, j) = \begin{cases} I_L^A(i, j) & \text{if } I_L^A(i, j) > I_L^B(i, j) \\ I_L^B(i, j) & \text{if } I_L^A(i, j) \leq I_L^B(i, j) \end{cases} \quad (3.1)$$

#### B. Fusion rule of higher sub band coefficients

The high pass sub band coefficients represent the detailed components of the source image; according to characteristic of HVS. So, it is easy to find that for the high resolution region the human visual interest is concentrated on the detection of changes in between regional contrast. Then spatial frequency measures in the overall activity an image is present. Therefore, we propose a scheme by computing the spatial frequency method in a neighbourhood to select the high frequency coefficients. The spatial frequency (SF), is originated from the HVS, indicates the overall active level in an image and measure the variation of pixels [9]. For an  $M \times N$  image  $I$ , with gray value  $I(i, j)$  at position  $(i, j)$  the spatial frequency is defined as

$$SF = \sqrt{(RF)^2 + (CF)^2} \quad (3.2)$$

Where RF and CF are the row frequency and column frequency respectively:

$$RF = \sqrt{\frac{1}{MN} \sum_{i=1}^M \sum_{j=1}^N [I(i, j) - I(i, j-1)]^2} \quad (3.3)$$

$$CF = \sqrt{\frac{1}{MN} \sum_{i=1}^M \sum_{j=1}^N [I(i, j) - I(i-1, j)]^2} \quad (3.4)$$

Each image is partitioned into  $B \times B$  blocks. The said blocks value varies according to the interest of the user, we consider  $8 \times 8$  as a block size to obtain more accurate values. Then, compare the spatial frequencies of two corresponding coefficient values in each block of  $I_{HIGH}^A$  and  $I_{HIGH}^B$  to construct the new block of fused image  $I_{HIGH}^F$ .

$$I_{HIGH}^F(m, n) = \begin{cases} I_{HIGH}^A(m, n) & \text{if } SF_{HIGH}^A > SF_{HIGH}^B \\ I_{HIGH}^B(m, n) & \text{if } SF_{HIGH}^A < SF_{HIGH}^B \\ \frac{I_{HIGH}^A(m, n) + I_{HIGH}^B(m, n)}{2} & \text{otherwise} \end{cases} \quad (3.5)$$

The Proposed method has accomplished the following Steps:

- 1) Decompose the source images A and B into low frequency sub band and a series of high frequency sub bands at L levels by using various Multi scale transforms.
- 2) Fuse the low frequency sub band coefficients and high frequency sub band coefficients according to lower sub band fusion rule and higher sub band fusion rules.
- 3) Reconstruct the original image based on the new fused coefficients of sub bands by taking respective inverse Multi scale Transform, thus fused image is obtained.
- 4) Compare the obtained fused image from various transforms with different evaluation parameters from equation.

#### IV. EXPERIMENTAL RESULTS AND ANALYSIS

To evaluate the performance of the multi scale transforms, several experimental results are presented in this section. Experiments are performed on multisource images MRI & CT. Similarly the CT and MRI images are taken from a doctor to study live case. The proposed method is applied to these image sets. To show the effectiveness of the multi scale transform the comparisons start with DWT [7-8], Contourlet Transform[5] and Non subsampled contourlet transform in transform domain techniques. The fused image output based on different methods is shown from Fig 6.

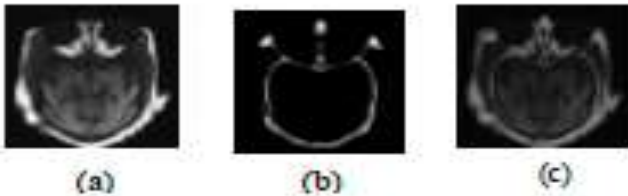


Fig. 6: MRI-CT fusion Results (a) Source Image (MRI)(b) Source Image(CT) (c) Fused Image.

##### A. Peak Signal to Noise Ratio (PSNR)

PSNR (Peak Signal to Noise Ratio) is a metric for the ratio between the maximum possible power of a signal and power of corrupting noise that affects the fidelity of its representation. It is used to measure the quality of reconstructed images.

$$PSNR = 10 \log_{10} \left( \frac{L^2}{M \times N \sum_{i=1}^M \sum_{j=1}^N (R(i,j) - I^F(i,j))^2} \right) \quad (4.1)$$

Where  $R_{(i,j)}$  and  $I^{F(i,j)}$  are the pixel values of the ideal reference and the obtained fused image, respectively. M and N are the dimensions of the images.

##### B. Mutual Information (MI)

Mutual information of two random variables is a quantity that measures the mutual dependence of the two variables. Here, MIRIF measures the information that reference and the fused image shares:

$$MI_{RI^F} = \sum_{i=1}^L \sum_{j=1}^L P_{RI^F}(i,j) \log_2 \frac{P_{RI^F}(i,j)}{P_R(i)P_{I^F}(j)} \quad (4.2)$$

Where  $P_{RI}$  is the normalized joint gray level histogram of images R and  $I^F$ ,  $P_R$  and  $P_{I^F}$  are the normalized marginal histograms of the two images.

The mutual information  $I_{AF}$  between the sources images A and the fused images F is defined as follows:

$$I_{AF} = \sum_{AF} P_{AF}(a,f) \log \frac{P_{AF}(a,f)}{P_A(a)P_F(f)} \quad (4.3)$$

Where PAF is the jointly normalized histogram of A and F, PA and PF are the normalized histogram of A and F, and a f represent the pixel value of the image A and F, respectively. The mutual information IBF between the source image B and the fused image F are similar to IAF. The mutual information between the source images A, B and the fused image F is the sum of IAF and IBF, i.e.

$$MI_F^{AB} = I_{AF} + I_{BF} \quad (4.4)$$

##### C. Gradient and Wrap

The gradient value and wrap values are facilitate the correlation between the resultant F and reference R images. If gradient value is high and wrap value is low then the two images are more correlated. The gradient and warp are defined as follows:

$$Grad = \frac{1}{M * N} \frac{\sum \sum \sqrt{[F(i,j) - F(i+1,j)]^2 + [F(i,j) - F(i,j+1)]^2}}{\sqrt{2}} \quad (4.5)$$

$$Wrap = \frac{1}{M * N} \sum_{i=1}^M \sum_{j=1}^N F(i,j) - R(i,j) \quad (4.6)$$

Where, M and N are size of the image.

#### V. EFFECTIVE GREAT DEGREES

This is because that the metrics QAB/F and Q0 mainly measure the amount of salient information transferred from source images into the fused image [Ref.10]. The metric QAB/F is defined as follows:

$$Q^{AB/F} = \frac{\sum_{n=1}^N \sum_{m=1}^M (Q^{AF}(n,m)W^A(n,m) + Q^{BF}(n,m)W^B(n,m))}{\sum_{n=1}^N \sum_{m=1}^M (W^A(n,m) + W^B(n,m))} \quad (4.7)$$

The dynamic range of  $Q^{AB/F}$  is [0, 1], and it should be as close to 1 as possible.

Another metric  $Q_0$  is as follows:

$$Q_0(A,F) = \frac{2\sigma_{af} \overline{af}}{(\sigma_a^2 + \sigma_f^2)(\overline{a}^2 + \overline{f}^2)} \quad (4.8)$$

Where  $\sigma_{af}$  represents the coherence between A and F,  $\sigma_a$   $\sigma_f$  denote the standard deviation of A and F;

$\overline{a}$ ,  $\overline{f}$  Represent the mean value of A and F respectively, similarly calculate  $Q_0(B,F)$  using above equation then finally the  $Q_0$  value is as follows:

$$Q_0 = \frac{Q_0(A,F) + Q_0(B,F)}{2} \quad (4.9)$$

The  $Q_0$  range is  $-1 \leq Q_0 \leq 1$  and it should be also as close to 1 as possible.

##### A. Correlation

It computes the correlation coefficient between fused images F and reference image R to computes the correlation coefficient using following equation:

$$COFF = \frac{\sum_{i,j} (F(i,j) - \overline{F})(R(i,j) - \overline{R})}{\sqrt{(\sum_{i,j} (F(i,j) - \overline{F})^2) (\sum_{i,j} (R(i,j) - \overline{R})^2)}} \quad (4.10)$$

Where  $\overline{F}$  and  $\overline{R}$  are mean value of fused and reference images respectively.

Appendix A: Performance Analysis Table

Algorithm	Mean	Standard deviation	Entropy	Gradient	Wrap	PSNR
DWT	59.26	ss9.42	6.68	10.56	-1.38	21.19
FDCT	59.93	59.81	6.79	6.02	0	25.26
Contourlet	60.13	60.44	10.4	10.4	0	25.63
NSCT	59.96	60.51	6.73	10.20	0.98	25.95

Table: I Evaluation of different methods for CT-MRI images

## VI. CONCLUSION

In this paper, performance analysis is compared with different multi scale transforms for the fusion of multi-modality images. The fusion procedure is discussed with different subband fusion rules to obtain fused image from different multi sources. The obtained fusion results are compared with different evaluation parameters. Finally those compared with DWT, Contourlet, Fast Discrete Curvelet [14] and NSCT fusion methods. We calculated and analyzed tools such as; PSNR, MI, Effective great degrees, gradient, wrap, standard deviation, mean and entropy values.

## REFERENCES

[1] G. Eason, B. Noble, and I. N. Sneddon, "On certain integrals of Lipschitz-Hankel type involving products of Bessel functions," *Phil. Trans. Roy. Soc. London*, vol. A247, pp. 529–551, April 1955. (references) Sabalan Daneshvar, Hassan Ghassemian, MRI and PET Image Fusion by Combining HIS and retina – inspired Models, *Information Fusion* 11, 2010, pp.114-123.

[2] Ch. Hima Bindu, Dr. K. Satya Prasad, "MRI-PET medical image fusion by combining DWT and contourlet Transform", To be published in springer conference, Aug2012, ITC 2012,LNEE,pp. 124-129, 2012.

[3] Guest Editorial, Image Fusion: Advances in the State Of The Art, *Information Fusion* 8, 2007, pp.114-118.

[4] Xiangzhi Bai, Fugen Zhou, Bindang Xue, Edge Preserved Image Fusion Based on Multiscale Toggle Contrast Operator, *Image And Vision Computing* 29, 2011, pp. 829-839.

[5] L.Yang, B.L.Guo, W.Ni, Multimodality Medical Image Fusion based on Multiscale Geometric Analysis of Contourlet Transform, *Neurocomputing* 72, 2008, pp. 203-211.

[6] G.G.Bhutada, R.S.Anand, S.C. Saxena, Edge Preserved Image Enhancement using Adaptive Fusion of Images Denoised By Wavelet And Curvelet Transform, *Digital Signal Processing* 21 (2011) 118-130.

[7] I.Pitas, *Digital Image processing Scheme and Application*, john wiley & sons. New York, 2000.

[8] A.Soma Sekhar, Dr.M.N. Giri Prasad, A Novel Approach Of Image Fusion On MR And CT Images

Using Wavelet Transforms, *Proc. Of IEEE ICECIT 3rd International Conference*, July 2011, pp. 172-176.

[9] Shutao Li, Bin Yang, Jianwen Hu, Performance comparison of Multi resolution transform for image fusion, *Information Fusion* 12, 2011, pp.74-84.

[10] Ch.Hima Bindu, et al, "Discrete Wavelet Transform Based Medical Image Fusion using Spatial Frequency Techniques", *International Conference on Recent Advances in Engineering and Technology(ICRAET 2012)*, Apr 2012.

[11] Arthur L.da Cuncha, JIANPING Zhou, "The Nonsubsampled Contourlet transform: Theory, Design and Applications." *IEEE Transactions on Image Processing*, Vol. 15, Oct2006.

[12] Ch.Hima Bindu, et al, "Multimodal Medical Image Fusion of MRI-PET using wavelet Transform ", *International Conference on Advance in Mobile Network, Communication and Its Application* Aug,2012.

[13]Xiaoqing Zhang, Yongguo Zheng, Yanjun Peng, Weike Liu, Changqiang Yang, Research on multi-mode medical image fusion algorithm based on wavelet transform and edge characteristics of images, *2nd International conference on Image and signal processing*, 2009, pp.1-4.

[14]Candès, L. Demanet, D. Donoho, L.X. Ying, Fast discrete curvelet transforms, *SIAM Multiscale Modeling and Simulation* 5 (3) (2006) pp: 861–899.

[15]Yi Chai, Huafeng Li, Xiaoyang Zhang, Multifocus Image Fusion based on features Contrast of Multiscale products in nonsubsampled Contourlet Transform Domain, *Optik* 123 2012, pp.569-581.

[16] J. Wenjun Chi, Sir Michael Brady, Niall R. Moore and Julia A. Schnabel, "Fusion of Perpendicular Anisotropic MRI Sequences", *2011 IEEE Int. Symp. on Biomedical Imaging (ISBI 2011)*, March30 – April 2 2011, Chicago, pp 1455-1458.